J Mater Sci (2011) 46:429–437
DOI 10.1007/s10853-010-4884-7

TEM analysis of diffusion brazement microstructure in a Ni_3Al-based intermetallic alloy

H. R. Zhang · A. Ghoneim · O. A. Ojo

Received: 18 June 2010 / Accepted: 28 August 2010 / Published online: 14 September 2010

Abstract Transmission electron microscopy study of brazed joint microstructure in a Ni_3Al-based intermetallic alloy IC 6 was performed. A continuously distributed microconstituents consisting of γ solid-solution, M_3B_2-type and $M_{23}B_6$-type borides, which were likely formed by eutectic-type reaction(s) from residual liquated insert during cooling from brazing temperature, were observed along the joint centreline. Consideration of possible incipient melting due to eutectic-type transformation reaction of these phases is pertinent to development of post braze heat treatment for modifying the brazement microstructure.

Introduction

The quest to increase the efficiency of the next generation aero-engines and to reduce their emissions has led to a search for heat resistant metallic materials that are lighter, stronger and with higher temperature capability than conventional nickel-based superalloys that have nearly reached their upper temperature limit of application. Intermetallic-based alloys and compounds, including titanium aluminides, nickel aluminides and refractory aluminide and silicide compounds, have evolved as prime alternate materials in this regard, and have been the subject of intense study for the past few decades. Their application, however, is contingent on the development of appropriate joining techniques during fabrication and repair of service-damage engine components. A substantial body of research on the fusion welding of intermetallics [1–5], has shown that while such high-energy beam-welding techniques as electron-beam and laser-beam welding are attractive for joining these materials, their application is severely limited by the high susceptibility of the materials to cracking during welding. Among the most investigated of the various intermetallics for commercial applications are the Ni_3Al-based alloys. A directionally solidified (DS) Ni_3Al-based alloy IC 6 has been developed at the Beijing Institute of Aeronautical Materials as a high-temperature structural material for manufacturing advanced jet-engine components. It has been tested successfully as a turbine-vane material in two different types of aero-engines [6]. It exhibits superior creep-rupture resistance properties, and can withstand higher temperatures (1050–1100 °C) than the majority of the currently used nickel-based superalloys. Studies have shown that the alloy is extremely difficult to weld due to its high susceptibility to severe weld cracking [4, 5]. Brazing has evolved is an alternate procedure for joining difficult-to-weld heat resistant alloys, due to both technological and economical factors [7–11]. Nonetheless, high temperature performance of brazed components is controlled by the nature of microstructural changes within the component during joining. An effective way of improving high temperature properties of brazed materials involves application of appropriate post braze heat treatment (PBHT) to modify as-brazed microstructure and impart desirable performance. Proper selection of suitable

H. R. Zhang
National Institute for Nanotechnology,
Edmonton T6G 2M9, Canada

A. Ghoneim · O. A. Ojo (✉)
Department of Mechanical and Manufacturing Engineering,
University of Manitoba, Winnipeg, Manitoba R3T 5V6, Canada
e-mail: ojo@cc.umanitoba.ca

PBHT is, however, dependent on adequate knowledge of the type of microconstituent phases formed in as-brazed material during joining. The objective of the present study was, therefore, to perform a careful transmission electron microscopy study to determine the nature of microconstituents formed in brazed joint of DS intermetallic alloy IC 6, with the use of a commercial filler alloy. This was aimed at contributing to the development of suitable PBHT for the material.

Materials and experimental procedure

The base material used in the study was DS alloy IC 6 with chemical composition of Ni–15.9Al–7.78Mo–1.18B (at.%). The filler alloy used was a metallic glass foil MBF 80 with a composition of 14.4Cr, 16.2B, 0.12C balance Ni (at.%). The base alloy in the form of 8 × 9 × 12 mm test coupons was sectioned from as-received plates by using a numerically controlled wire electro-discharge machine (EDM). Brazing was carried out in a LABVAC II brazing furnace under a vacuum of 10^{-4} to 10^{-5} torr at 1100 °C for 1 h. The bonded specimens were sectioned using the EDM and prepared by standard metallographic techniques for microstructural study. The specimens were etched in a solution of 10 mL HF + 45 mL HNO_3 + 45 mL H_2O at 6 V for 5 s. Preliminary general assessment of the joint microstructure was performed by an inverted-reflected light microscope equipped with a CLEMEX Vision 3.0 image analyzer. Scanning electron microscopic examination using secondary and backscatter electron imagine modes and compositional analysis of joint were conducted by a JEOL JSM-5900LV scanning electron microscope equipped with an ultra-thin window Oxford energy dispersive spectrometer (EDS) system and INCA software. In addition, thin foil specimens for transmission electron microscopy (TEM) study of microconstituent phases in the brazed joint region were also sectioned from the transverse section of the joint. The foils were prepared by mechanical polishing and dimpling to a thickness of less than 10 μm followed by ion milling in a Gatan precision ion polishing system (PIPS). TEM microchemical and crystal structure analyses were performed in a field emission gun JEOL 2100F scanning transmission electron microscope equipped with an Oxford ultra-thin window energy dispersive spectrometer, electron energy loss spectrometer and Gatan imaging filter (GIF) system. X-ray microanalysis by energy dispersive spectroscopy (EDS) in the transmission electron microscope was performed using theoretical Cliff-Lorimer k factors and electron energy loss spectroscopy (EELS) spectra were collected with 0.5 eV/channel dispersion.

Results and discussion

Figure 1 is a low magnification optical micrograph that shows, in general, the brazed joint microstructure consisting of a continuously distributed centreline eutectic-like

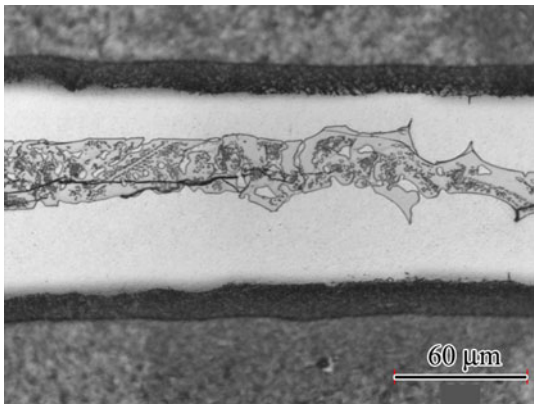

Fig. 1 An optical microscopy image of brazed joint showing a centreline eutectic-like microconstituent

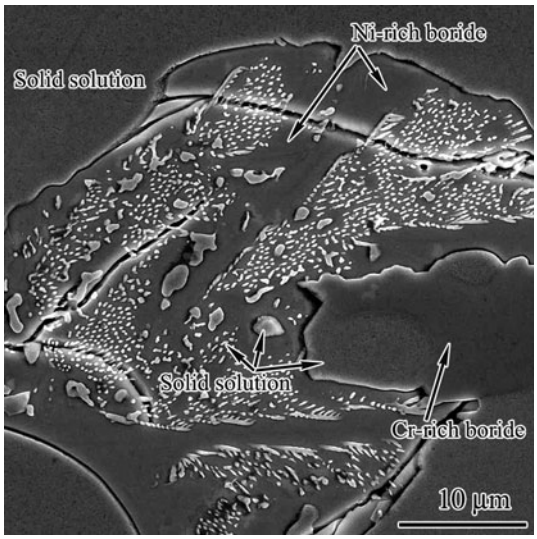

Fig. 2 SEM micrograph of the eutectic-like microconstituent containing different second-phase particles

Table 1 Average metallic composition of centerline eutectic product as determined by SEM–EDS

Phase	Composition (at.%)			
	Cr	Al	Mo	Ni
Cr-rich boride	66.54	–	19.11	14.35
Ni-rich boride	10.45	1.47	–	88.08
Ni solid solution	13.28	1.78	–	84.94

microconstituent. A SEM higher magnification micrograph of the microconstituent in Fig. 2 shows that it consists of different second-phase particles, most of which are too small to enable reliable SEM–EDS chemical composition analysis. Nonetheless, preliminary EDS semi-quantitative analysis suggested the presence of three phases, one Cr-based phase and two Ni-based phases (Table 1). TEM analysis was used to perform unambiguous identification of the phases and a bright-field TEM image of a section of the microconstituent is shown in Fig. 3a. Micro-chemical X-ray analysis of the eutectic-like microconstituent by TEM-EDS confirmed the occurrence of two chemically similar phases in terms of been primarily rich in Ni, with some Cr and marginal content of Mo (Fig. 3b). Nevertheless, due to inherent limitation of the EDS to adequately analyze B, an advanced electron spectroscopy technique, EELS, which is more sensitive to light elements with higher energy resolution, was used to chemically discriminate between the two Ni-rich phases. Careful EELS analysis showed that one of the two phases contains B while the other is essentially B-free (Fig. 3c). TEM electron diffraction analysis was subsequently performed to study the crystal structure of the phases. The B-free Ni-rich phase was found to be Ni-based solid solution phase, γ, with face centered cubic (fcc) crystal structure. The B-bearing phase, which constitutes the matrix phase of the centreline eutectic-like microconstituent (Fig. 3a), was found to exhibit a complex fcc crystal structure. Analysis of selected area electron diffraction patterns (SAEDPs) obtained from different zone axes (Fig. 4a–c) indicated that phase is based on $M_{23}B_6$ boride (M: Ni, Cr, Mo) with a lattice parameter $a = 1.06$ nm, similar to that of $Ni_{23}B_6$. To the knowledge of the authors, this phase has not been previously reported in alloy IC 6. TEM-EDS and EELS analyses performed on the Cr-based phase indicated that the phase to be rich Cr with some Mo and Ni (Fig. 5a–c). SAEDPs obtained from three systematically tilted

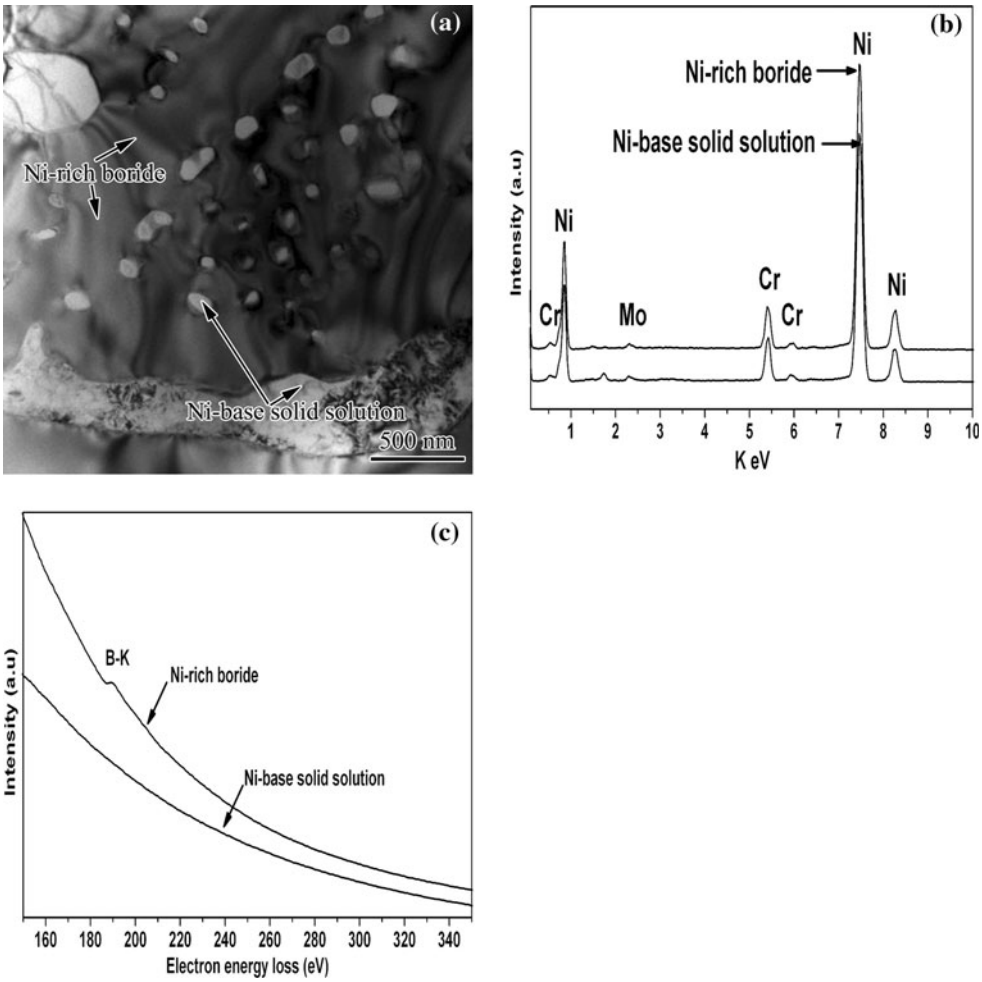

Fig. 3 **a** TEM bright-field image showing the two nickel-based phases in the centreline eutectic-like microconstituent **b** EDS spectral and **c** EELS spectra from the phases

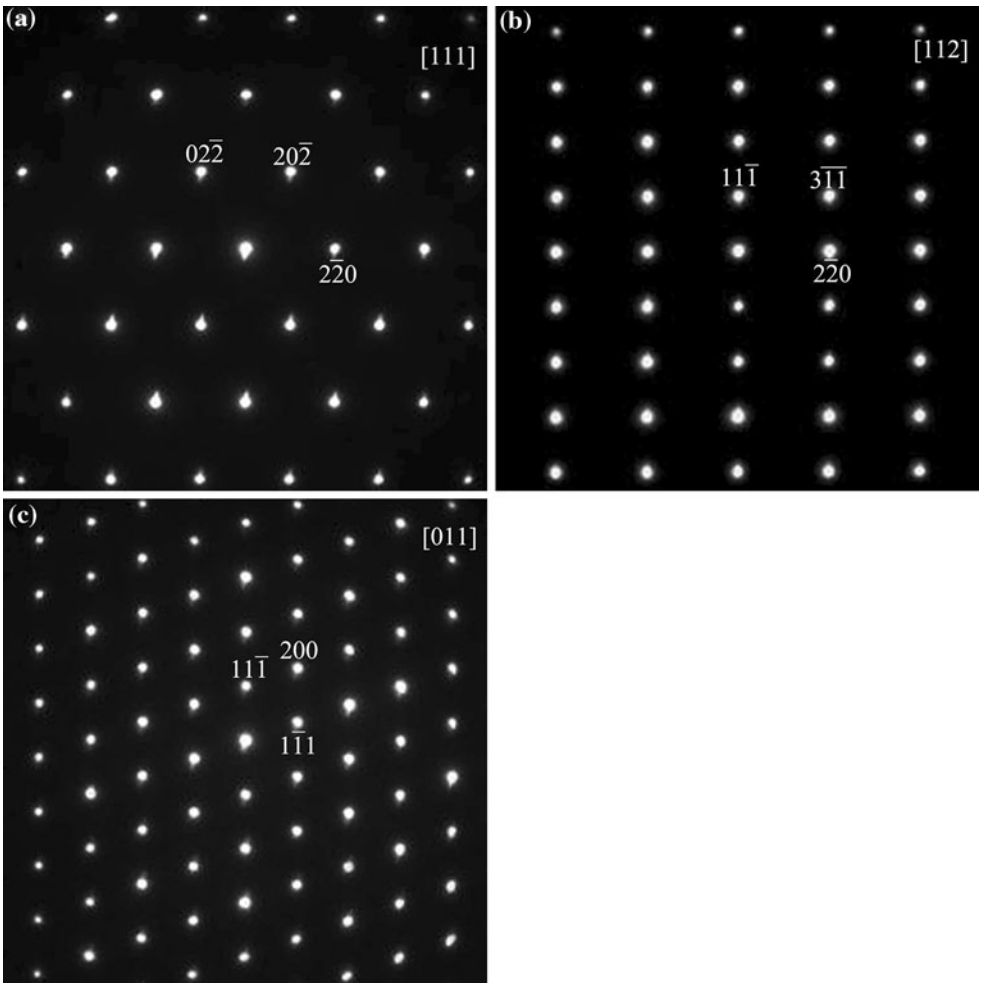

Fig. 4 Selected area electron diffraction patterns from **a** [111], **b** [112] and **c** [011] zone axes of the $M_{23}B_6$ boride phase

zone-axes in a particle of the phase are shown in Fig. 6a–c. Careful analysis of the electron diffraction patterns showed that this phase is based on M_3B_2 (M: Cr, Mo, Ni), with a primitive tetragonal crystal structure and lattice parameters $a = 0.59$ nm, $c = 0.31$ nm and $c/a = 0.54$, similar to those of Cr-rich M_3B_2 borides reported in nickel-based superalloy. The distribution of B in the three main phases within the centreline eutectic-like microconstituent was further investigated by using EELS-based energy-filtered TEM (EFTEM) imaging technique. Figure 7a is a zero-loss EFTEM image of the Cr-rich boride, Ni-based solid solution and Nickel-rich boride. The B-map (Fig. 7b), Cr-map (Fig. 7c) and Ni-map (Fig. 7d) images confirmed that while B is present in the M_3B_2 and $M_{23}B_6$ borides, the γ solid solution is depleted in B.

During diffusion brazing, a filler alloy, sandwiched between two substrates to be joined, melts and rapidly attains equilibrium at liquid–solid base alloy interfaces through a dissolution process. Following this, a solid-state diffusion of melting point depressant element occurs from the liquid interlayer to the solid substrate. This results in reduction in the volume of liquid that can be maintained at equilibrium, causing isothermal solidification to proceed inward from the liquid–solid interfaces. Insufficient brazing time to allow complete isothermal solidification process would cause the residual liquid insert to transform during cooling from the joining temperature into non-equilibrium solidification products, often by eutectic-type transformation. A schematic of the liquidus projection of the nickel rich portion of Ni–Cr–B ternary phase diagram according to Villars et al. [12] is shown in Fig. 8. According to the diagram, nickel rich and chromium rich borides can form by monovariant eutectic-type reaction. The lowest solidification temperature in the system is at point E_2 on the diagram, where solidification terminates by an invariant ternary eutectic reaction to produce nickel rich

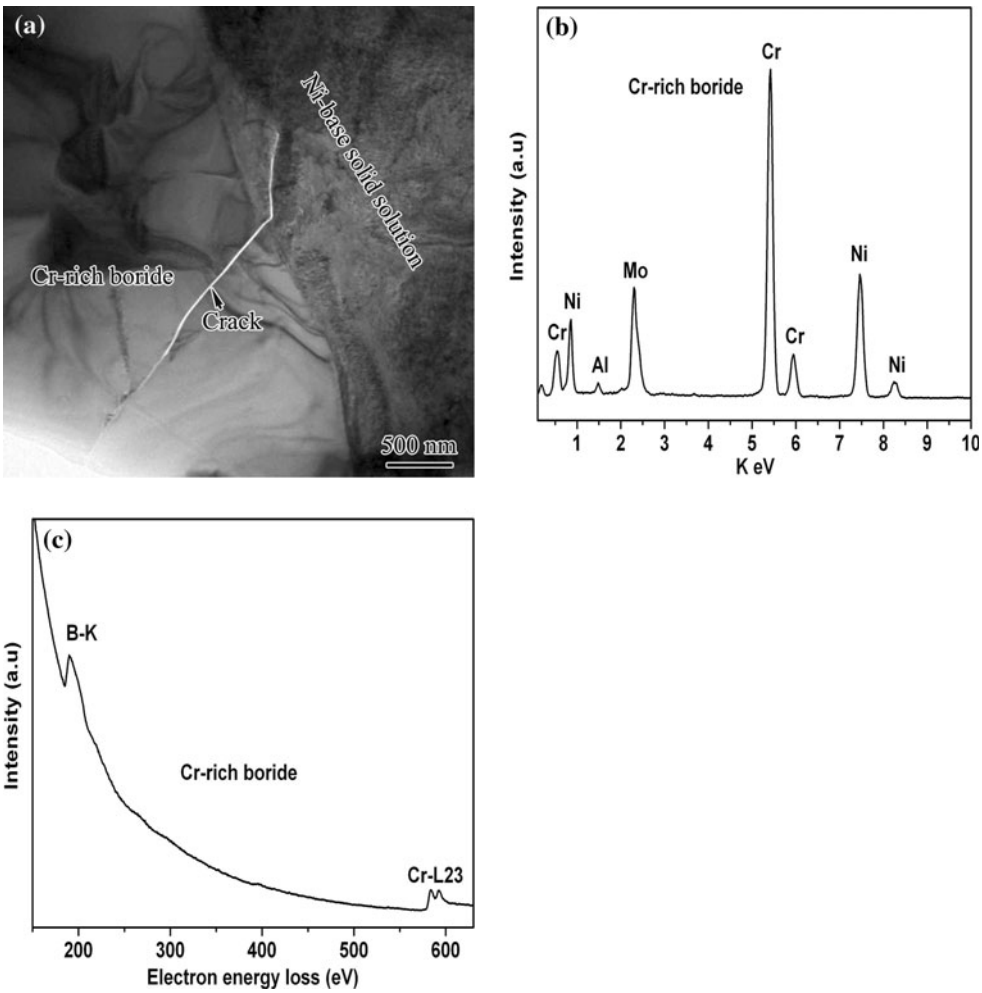

Fig. 5 **a** TEM bright-field image showing the Cr-based phase in the centreline eutectic-like microconstituent **b** EDS spectral and **c** EELS spectra from the phase

boride phase, chromium rich boride phase and nickel rich solid solution. The terminal solidification temperature is below the bonding temperature used in the present study. Moreover, the solidification transformation behaviour of residual liquid during bonding of pure nickel using a Ni–B–Cr ternary filler alloy was studied by Ohsasa et al. [13]. Their simulation results showed that during solidification of the residual liquid in a sample held at 1100 °C, Ni-rich γ phase formed as the primary phase, followed by the eutectic reaction $L \rightarrow \gamma + Ni_3B$ at 1042 °C. Solidification was reported to be completed with a ternary eutectic reaction $L \rightarrow \gamma + Ni_3B + CrB$ at 997 °C. Therefore, the centerline eutectic-like microconstituent observed in the present work, consisting of γ, M_3B_2 and $M_{23}B_6$, is believed to be formed by eutectic-type solidification reaction(s) during cooling, due to an insufficient holding time for complete isothermal solidification during bonding. Formation of this eutectic-type product with continuously distributed morphology can be deleterious to mechanical properties, as it may provide a low resistance path for crack initiation and/or propagation. Crack was indeed observed to have propagated through the eutectic (Fig. 5a). Generally, post braze heat treatment (PBHT) is often used to modify brazement microstructure to eliminate deleterious constituents and improve mechanical properties. However, based on the result of this study, if exclusive solid-state microstructural modification is required by PBHT, careful selection of PBHT temperature is imperative, as undesirable incipient melting could occur above the ternary eutectic temperature of the brazement. Further study to determine this critical temperature, using Differential Scanning Calometry analysis, as well as examination of microstructural response to heat treatments below and above this temperature is deemed pertinent to proper selection of suitable PBHT for the alloy.

In addition to the centerline eutectic, fine lath-shaped particles were formed within the base-alloy region adjacent to the brazed joint (Figs. 1a, 9a). Microanalysis by

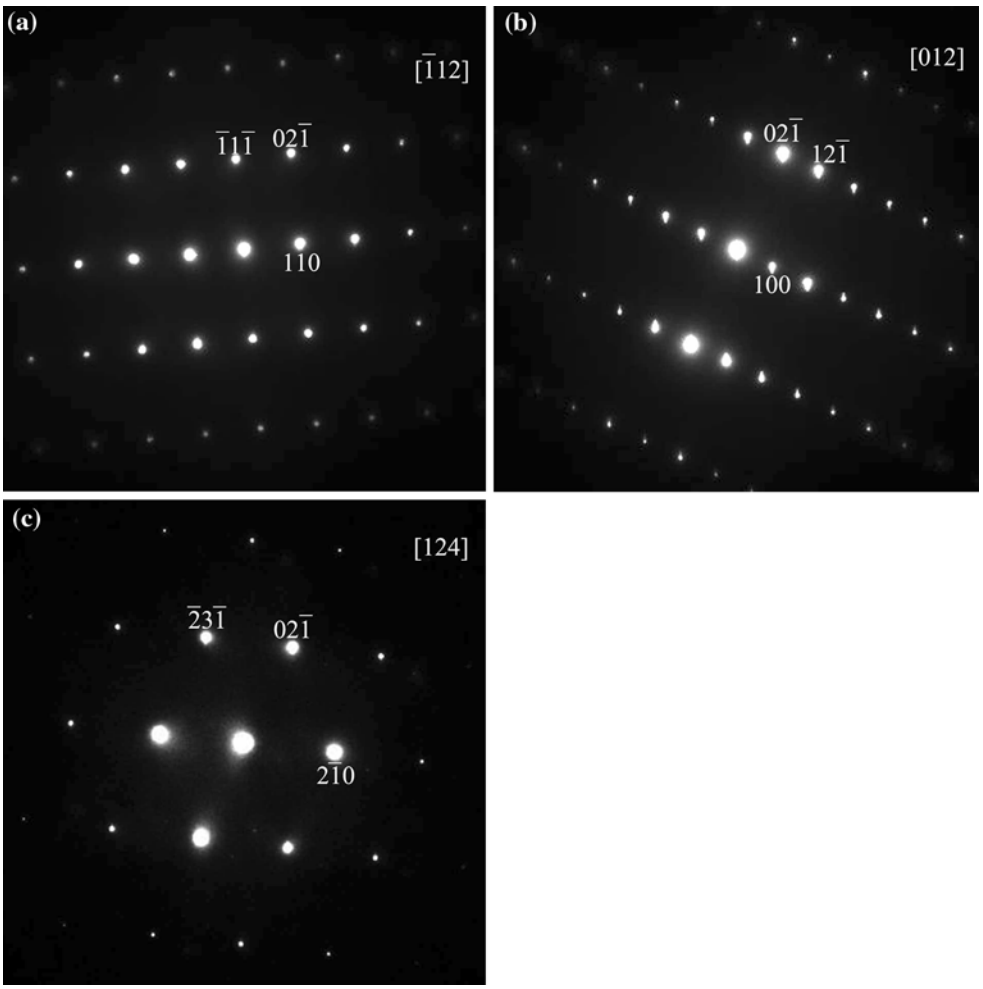

Fig. 6 Selected area electron diffraction patterns from **a** [$\bar{1}$12]], **b** [012] and **c** [124] zone axes of the tetragonal M_3B_2 (M: Cr, Mo, Ni) boride phase

TEM-EDS and EELS suggested that the precipitates are Ni-Mo boride (Fig. 9b–d). Analysis of SADPs that were obtained by systematically tilting a particle of this phase to three different zone axes (Fig. 10a–c) showed that the phase is based on M_3B_2-type boride (M: Ni, Mo) with orthorhombic crystal structure and lattice parameters $a = 0.74$ nm, $b = 0.47$ nm and $c = 0.31$ nm. Similar observation of precipitation of second-phase particles in region adjacent to substrate/joint interface has been made in other alloy systems [14, 15]. The interface orthorhombic (Ni, Mo)$_3B_2$ borides are different from the tetragonal M_3B_2 borides formed within the joint centreline eutectic in terms of their chemical composition, the orthorhombic M_3B_2-type borides are essentially Cr-free while the tetragonal M_3B_2-type borides are relatively rich in Cr. Addition of Cr and V has been reported to result in transformation of orthorhombic M_3B_2 (M: Mo, Ni) to tetragonal M_3B_2 (M: Mo, Ni, Cr,V) in a Mo–Ni–B based alloy [16]. The location, size, morphology and distribution of the precipitates suggest that they form by solid-state reaction within the base-alloy due to diffusion of B from the liquated filler alloy into the substrate during joining. Ojo et al. [17] have observed and reported that the growth of similar precipitation zone in a brazed nickel-based alloy seemed to follow a parabolic relationship with holding time, suggesting that the precipitate formation is diffusion controlled. If the presence of the interface (Ni, Mo)$_3B_2$ borides observed in the present work, presumably formed by solid-state reaction, is determined to be detrimental to properties of brazed material, as it has been found in other materials, it may be possible to eliminate them by solid-state dissolution reaction by suitably chosen PBHT. Nevertheless, development of such suitable PBHT to modify the brazement microstructure, exclusively in the

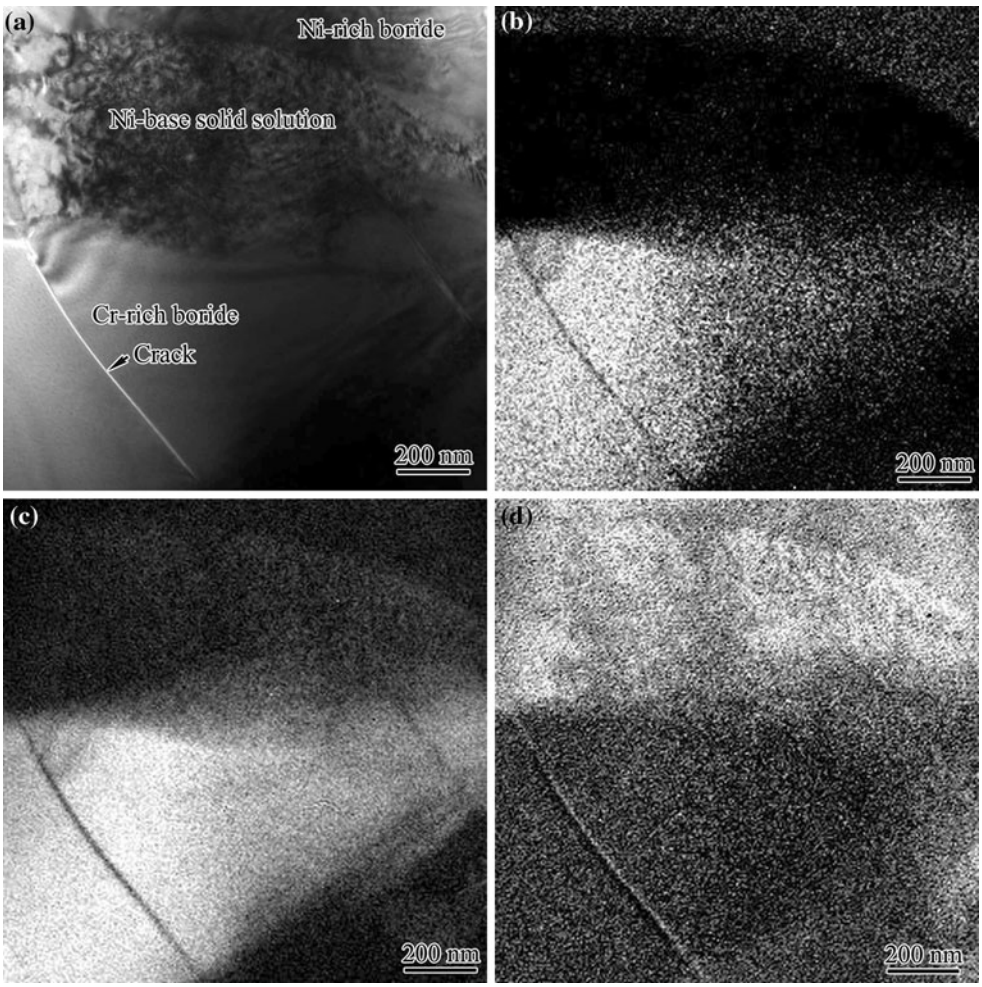

Fig. 7 Energy-filtered TEM images of the centreline eutectic-like microconstituent **a** Zero-loss, **b** B-map, **c** Cr-map and **d** Ni-map

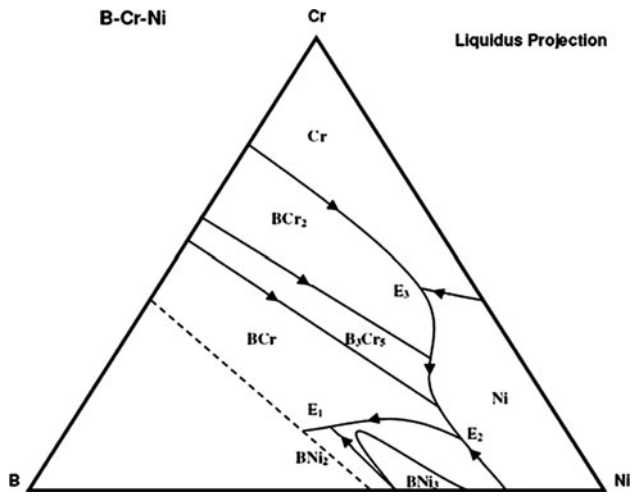

Fig. 8 Schematic of the liquidus projection of Ni–Cr–B ternary system [12]

solid-state, would require determination of the minimum liquation reaction temperature of the centreline eutectic that may induce undesirable incipient melting occurrence during heat treatment.

Summary and conclusion

Diffusion brazing of the alloy IC 6 resulted in formation of a centreline microconstituent consisting of γ, tetragonal M_3B_2 (M: Cr, Mo, Ni) and $M_{23}B_6$ (M:Ni,Cr,Mo) phases, which were likely formed by eutectic-type reaction (s) from residual liquated insert during cooling from brazing temperature. Fine lath-shaped M_3B_2 (M: Ni, Mo) borides, with orthorhombic crystal structure, were observed within the base-alloy region adjacent to the brazed joint. The particles were presumably formed by solid-state

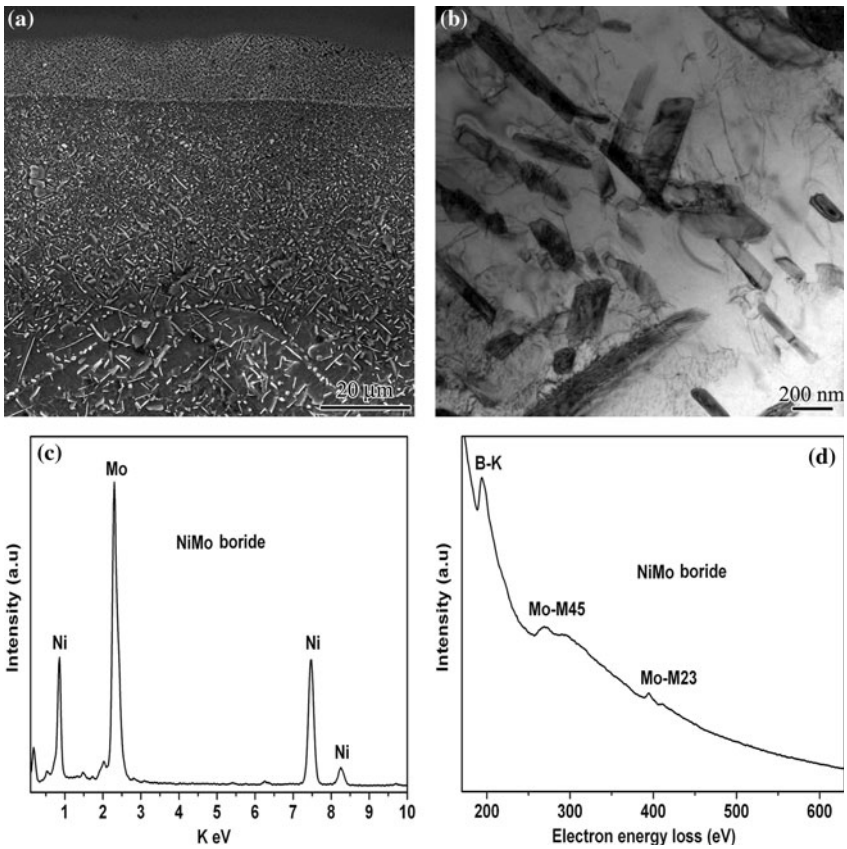

Fig. 9 **a** SEM micrograph of fine lath-shaped particles within base-alloy region adjacent to the brazed joint **b** TEM bright-field image **c** EDS spectra and **d** EELS spectra of the lath-shaped particles

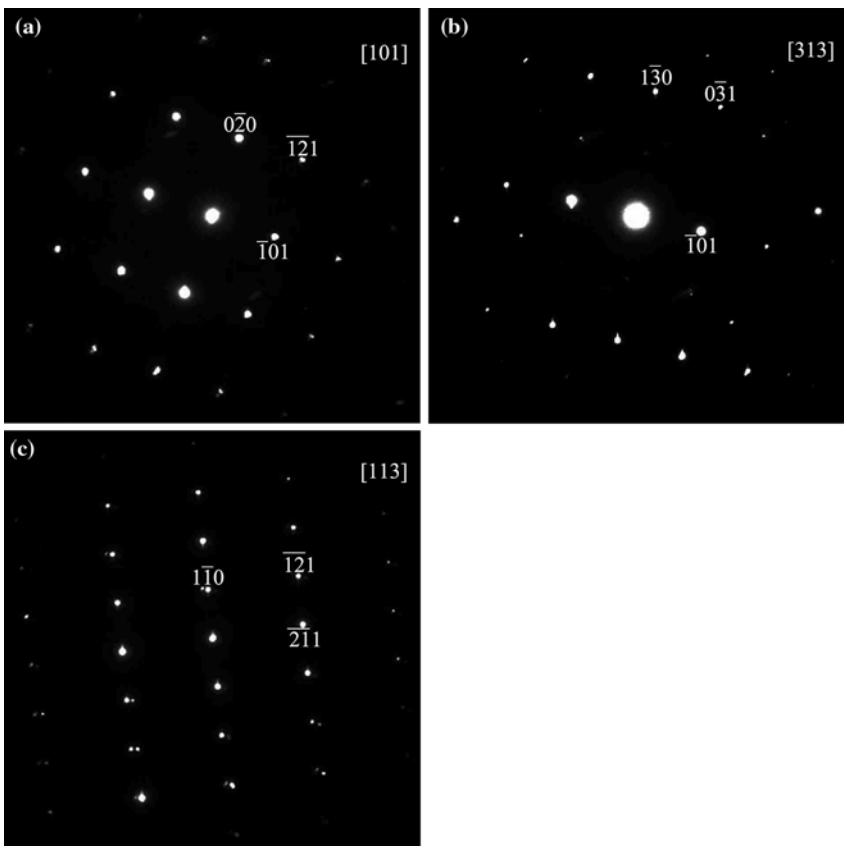

Fig. 10 Selected area electron diffraction patterns from **a** [101], **b** [313] and **c** [113] zone axes of the orthorhombic M_3B_2 (M: Mo, Ni) boride phase

precipitation reaction due to diffusion of boron from the liquated insert. Development of suitable PBHT to modify the brazement microstructure exclusively in the solid-state requires determination of the minimum liquation reaction temperature of the centreline eutectic that may induce undesirable incipient melting occurrence during heat treatment.

Acknowledgements Financial support from Natural Sciences and Engineering Research Council of Canada (NSERC) is gratefully acknowledged. Thanks also due to Dr. Y. F. Han of Beijing Institute of Aerospace Materials for providing alloy IC 6.

References

1. David SA, Jemian WA, Liu CT, Horton JA (1985) Weld J 64:22s
2. Molian PA, Yang YM, Srivatsan TS (1992) J Mater Sci 27:1857. doi:10.1007/BF01107213
3. Patterson RA, Martin PL, Damkroger BK, Christodoulou L (1990) Weld J 69:39s
4. Ojo OA, Ding RG, Chaturvedi MC (2006) Scripta Mater 54:2131
5. Ding RG, Ojo OA, Chaturvedi MC (2008) Intermetallics 15:1504–1510
6. Kong Z, Ji L, Han Y, Xu H (2007) Mater Sci Forum 546–549: 1443
7. Asthana R, Singh M, Sobczak N (2010) J Mater Sci 45(16):4276. doi:10.1007/s10853-010-4647-5
8. Singh M, Shpargel TP, Asthana R (2008) J Mater Sci 43(1):23. doi:10.1007/s10853-007-1985-z
9. Dezellus O, Voytovych R, Li APH, Constantin G, Bosselet F, Viala JC (2010) J Mater Sci 45(8):2080. doi:10.1007/s10853-009-3941-6
10. Singh M, Asthana R (2010) J Mater Sci 45(16):4308. doi: 10.1007/s10853-010-4510-8
11. Elrefaey A, Tillmann W (2010) J Mater Sci 45(16):4332. doi: 10.1007/s10853-010-4357-z
12. Villars P, Prince A, Okamoto H (1993) Handbook of ternary alloy phase diagrams. ASM International, Metals Park, OH
13. Ohsassa K, Shinimura T, Narita T (1999) J Phase Equilibria 20:199
14. Gale WF, Wallach ER (1991) Metall Trans A 22A:2451
15. Idowu OA, Ojo OA, Chaturvedi MC (2006) Metall Mater Trans A 37:2787–2796
16. Yamasaki Y, Yonetsu M, Takagi K (2000) J Jpn Soc Powder Powder Metall 47:521–525
17. Ojo OA, Richards NL, Chaturvedi MC (2008) Conference of Metallurgist (COM) August 24th–27th, Winnipeg, Canada